Advanced Composites and Hybrid Materials (2018) 1:577–590
https://doi.org/10.1007/s42114-018-0040-7

ORIGINAL RESEARCH

Chitosan biopolymer functionalized gold nanoparticles with controlled cytotoxicity and improved antifilarial efficacy

Pranesh Chowdhury[1] · Bishnupada Roy[1] · Niladri Mukherjee[2] · Suprabhat Mukherjee[2] · Nikhilesh Joardar[2] · Maloy Kr. Mondal[1] · Debiprasad Roy[1] · Santi P. Sinha Babu[2]

Received: 20 January 2018 / Accepted: 4 May 2018 / Published online: 31 May 2018

Abstract

Ultra-high stable chitosan functionalized gold nanoparticles (GNPs) of desired biopolymeric corona are synthesized without adding conventional hazardous reducing agents. The inherent unique set of properties like reducing ability, stabilizing effect, and mucoadhesiveness of chitosan is exhibited in the present work. Morphologies and ultra-stability of the synthesized materials are characterized by standard techniques. The mucoadhesiveness of the synthesized materials are well documented through the biological potency of the synthesized GNPs. The prominent bioactivity is evident from the antifilarial activity. The cellular and molecular level studies on the induction of oxidative stress, DNA damage, and undesirable protein expression clearly explain the antifilarial activities. Interestingly, the developed nanoparticle shows no detectable sign of toxicity when evaluated in vitro (rat peritoneal MΦ) or in vivo (Wistar rat). Therefore, the synthesized green GNPs appear to be a substantial promise as an efficacious broad-spectrum nanotherapeutic agent with safe outcome for clinical attempt.

Keywords Antifilarial activities · Biopolymer · Chitosan · Cytotoxicity · Gold nanoparticles · Mucoadhesiveness

1 Introduction

Chitosan is one of the most abundant natural biopolymers, obtained from chitin. Chemically, it is a random co-polymer of β-(1-4)-linked D-glucosamine and *N*-acetyl-D-glucosamine. The presence of hydrophilic hydroxyl groups makes the co-polymer suitable for super absorption of water [1]. The majorities of polysaccharides are normally neutral or negatively charged in an acidic environment. However, chitosan is positively charged in the same environment due to its amino groups. This distinct characteristic induces bioactivity of the chitosan. The other interesting features of chitosan are susceptibility to chemical modifications, biocompatibility, non-toxicity, low allergenicity, and biodegradability [2]. Many recent reviews [3, 4] focus on clinical use of chitosan-based composite (with quantum dots, nanoparticles, and carbon dots) and chitosan-mediated fabrication of metal nanocomposites for biomedical applications.

Lymphatic filariasis (LF), a vector-borne disease, is caused by filarial parasites *Wuchereria bancrofti*, *Brugia malayi*, and *Brugia timori*. As per report of WHO, it causes havoc mainly in tropical and subtropical countries due to favorable atmosphere for the growth of filarial parasites. The WHO initiated a drive to eliminate the filarial disease by 2020 [5]. Thus, the search for a new therapeutic solution against human lymphatic filariasis has emerged as a thrust-driven area of research.

Systemic chemotherapeutic targeting of filarial parasites is unfocused due to their deep-seated location in lymphatic vessels. Chourasia et al. [6] reported that the peculiarity of lymphatic vasculature underneath the subcutaneous layer of skin preferentially allows entry of only 10–100 nm-sized particles. Hence, out of several promising therapeutic modalities, exploiting metal nanoparticles for targeted apoptosis is considered as the effective means for treating the

Electronic supplementary material The online version of this article (https://doi.org/10.1007/s42114-018-0040-7) contains supplementary material, which is available to authorized users.

✉ Pranesh Chowdhury
pranesh_02@yahoo.co.in

[1] Polymer & Nano Research Laboratory, Department of Chemistry, Visva-Bharati University, Santiniketan, India

[2] Parasitology Laboratory, Department of Zoology (Centre for Advanced Studies), Visva-Bharati University, Santiniketan 731235, India

aforesaid pathogens. But there are very few reports on antifilarial activity of metal nanoparticles. Most of the works done so far are concerned on the efficacy of silver nanoparticles against mosquito larvae and the vector of malaria and filaria [7, 8]. Therefore, urgent development of therapeutics against filarial parasite is considered as the foremost agenda to the scientific community but at the same time cytotoxicity of the material should also be taken into consideration. Out of several promising approaches, polymer-modified metal nanoparticles are considered as the effective means for treating the aforesaid pathogens particularly the drug-resistant ones. Among the polymer-capped bioactive nanoparticles, silver and copper nanoparticles have especially engrossed major attention [9]. Goswami et al. [10] confirmed the filaricidal efficacy of silver nanoparticles with proof of apoptosis as a novel antifilarial rationale. Roy et al. [11] reported that the LD_{50} values of chitosan-stabilized silver nanoparticles for mf and adult of *Setaria cervi* were 12 and 13 μg/ml respectively. Ahmad et al. [12] synthesized copper(II) oxide nanoparticles to augment antifilarial activity of albendazole, a therapeutic benzimidazole. But major demerit of silver and copper nanoparticles is the cytotoxicity and genotoxicity on non-target tissues.

Suitable bioactivity with less cytotoxicity is always a desirable target for biochemists over the years. It is well known that gold is inert in the bulk and is only active as a catalyst in the form of nanoparticles. However, Carabineiro [13] reported that gold nanoparticles can have an important role, not only in catalysis, but also in nanomedicine including diagnostics, therapy, vaccine, and hygiene. Gold nanoparticles (GNPs), unlike silver nanoparticles, possess permissible cytotoxicity but at the same time their activities against diverse infectious agents including microfilaria are also found to be relatively low [14]. In this circumstance, surface functionalization of GNPs may be planned and executed in a more effective way for betterment of bioactivity. One such functionalization can be with chitosan, which enables its efficient interaction and permeation of cellular membranes, providing an effective adjuvant [15–20]. As both GNPs and chitosan have been shown to have low toxicity and high biocompatibility, their composite material should also be less cytotoxic and biocompatible.

The abovementioned literature survey motivates us to carry out surface modification by chitosan (a biopolymer), poly(vinyl alcohol) (PVA) (a non-biopolymer), and tyrosine (a biomolecule) for comparative analysis to develop promising bioactive nanoparticles with minimum cytotoxicity. The study emphasizes on the supremacy of biopolymer-inspired GNPs over others in terms of antifilarial efficiency and also its way of action through cellular and molecular level studies.

2 Materials and methods

2.1 Materials

Gold hydrochloride (Aldrich, USA), chitosan (practical grade, 75% deacetylated, Aldrich, Germany), polyvinyl alcohol (Burgoyne Burbidges and Co India Pvt. Ltd.), and L-tyrosine hydrochloride (Sigma Life Sciences, USA) were used as received and double-distilled water was used throughout. For cellular and molecular biology experiments, HPLC grade methanol, acetic acid, and other chemicals and solvents of highest purity grade were purchased from Merck, India. Milli-Q water (Milli-Q Academic with 0.22 μm Millipak R-40) was used throughout the study. De-ionized and nuclease-free water (Fermentas, India), FBS (fetal bovine serum), HEPES buffer, streptomycin, penicillin, amphotericin-B, RPMI-1640, and MTT (3-(4, 5-dimethyl-thiazol-2-yl)-2,5-diphenyl-tetrazolium bromide) were purchased from Sigma-Aldrich, St. Louis MO, USA. Agarose was obtained from Invitrogen (USA). Primary antibodies (EGL-1, CED-3, CED-4, and CED-9) and horseradish peroxidase (HRP) were purchased from Santa Cruz Biotechnology (Santa Cruz, CA). Anti-GAPDH antibodies were obtained from Bio Bharati Life Science Pvt. Ltd. (India). Polyvinylidene difluoride (PVDF) membranes were used for transferring the blots.

2.2 Instrumentation

UV-Vis spectrophotometer (Shimadzu, model UV-PC) was used for the detection of surface plasmon resonance of the samples. Sample for transmission electron microscopy (TEM) was prepared using carbon-coated copper grids in a JEOL TEM-2010 instrument. Scanning electron microscopy (Zeiss, model: Sigma) was used for surface morphology study; surface charge (ζ-potential) and size distribution (dynamic light scattering study) of the particles were carried out using Malvern Zeta-sizer Ver.6.34 instrument. Branson 1510 sonicator was used to obtain ultrasound of frequency 40 kHz. New Brunswick CO_2 incubator was used for parasite culture. Bio-Rad Mini protean electrophoresis system was utilized for SDS PAGE analysis. Genei horizontal gel system was used for DNA electrophoresis. Centrifugations of the samples were performed at 4 °C by REMI ultracentrifuge. Protein bands were visualized by a Gel Doc imaging system (Bio-Rad, USA). Cytotoxicity and apoptosis-specific double staining were monitored using an inverted phase-contrast microscope with fluorescence attachment (Dewinter, Italy). Cyclic voltammetry was carried out in an Auto lab instrument with a scan rate 100 mV/s.

Table 1 Preparation of composites

Sample	Composition		Wavelength (max) (nm)	Color	Stability
	Volume of 2.5% reducing agent (ml)	Volume of 10^{-3} M $HAuCl_4$ aqueous solution (ml)			
GNP-1	10.00; chitosan	10	523.0	Red	Medium
GNP-2	05.00; chitosan	10	521.0	Red	Medium
GNP-3*	02.50; chitosan	10	521.0	Red	High
GNP-4	01.25; chitosan	10	521.0	Red	Low
GNP_t	02.50; tyrosine	10	521.0	Red	Medium
GNP_p	02.50; poly(vinyl alcohol)	10	525.0	Red	Low

*GNP-3 is referred as GNP_c throughout the text

2.3 Chemical synthesis and stabilization of gold nanoparticles

Six sets of GNPs were synthesized by in situ reducing cum stabilizing technique using chitosan (a biomacromolecule), tyrosine (a biomolecule), and PVA separately with the help of ultrasound (40 kHz) as a greener energy source. The required solutions were placed in ultrasonic bath for 5 h at 70 °C until prominent color changes were noticed from colorless to red. UV-Vis spectral analysis was carried out to monitor the reaction by checking the SPR (surface plasma resonance) behavior of GNPs. After completion of conversion, the GNPs were purified by ultracentrifugation and re-dispersion in 1% acetic acid solution. Finally, the sample was stored in a cold dry place to check the stability. Quantitative conversion of Au(III) to Au(0) was verified by quantitative chemical analysis of Au(III) of the solution obtained after centrifugation by standard protocol [21].

2.4 Assessment of antifilarial activity

The developed chitosan containing material (GNP_c) was assayed for antifilarial activities at dose-dependent manner (3, 7.5, 15 μg/ml). The results were compared with chitosan solution (without GNP) and GNP synthesized by tyrosine (GNP_t) and PVA (GNP_p). (Experimental details are given as supplementary data.)

2.4.1 Collection and in vitro treatment of *Setaria cervi*

The collection and in vitro treatment of *S. cervi* (a filarial parasite) were performed as reported earlier [22, 23].

2.4.2 Trypan blue dye exclusion test

Mortality of exposed mf was checked by trypan blue dye exclusion method [24] after 24-h exposure and the results were expressed in percentages.

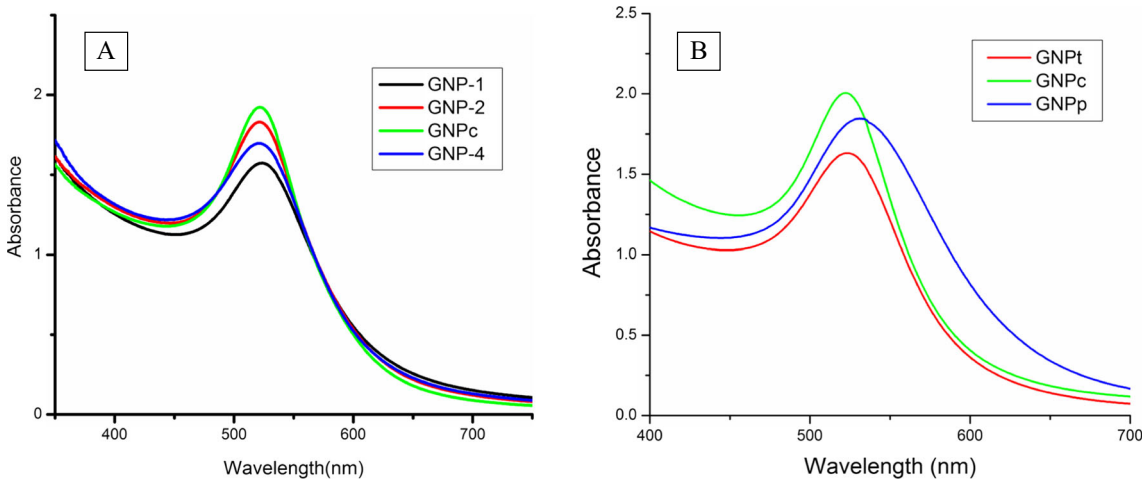

Fig. 1 **a**, **b** UV-Vis spectra of various GNP samples (GNP-1,2,3,4 represents gold nanoparticles produced by different proportions of chitosan polymer; GNP_c, GNP_p, and GNP_t stand for chitosan, PVA, and tyrosine-capped gold nanoparticle respectively)

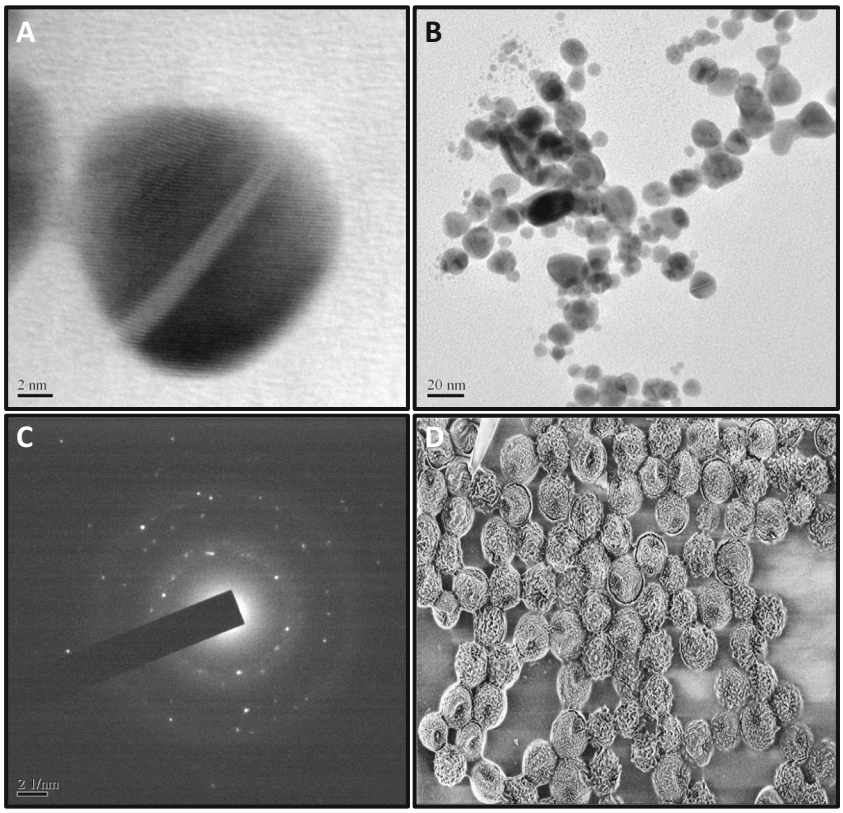

Fig. 2 Morphological analysis of the sample (GNP_c) by TEM (**a**, **b**) and SEM (**d**) and SAED (**c**) study

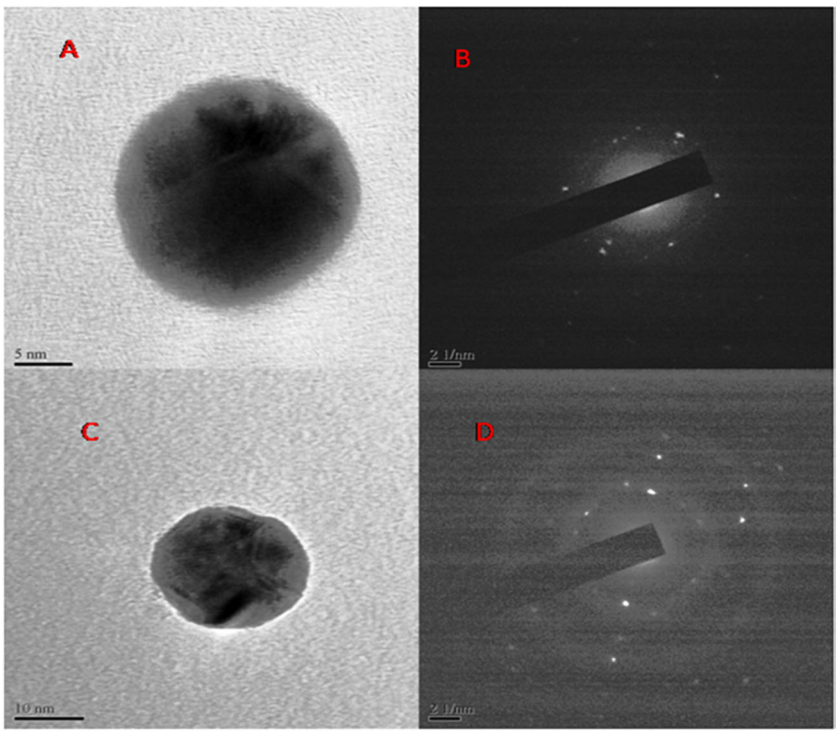

Fig. 3 TEM images of GNP_p (**a**) and GNP_t (**c**) and SAED images of GNP_p (**b**) and GNP_t (**d**)

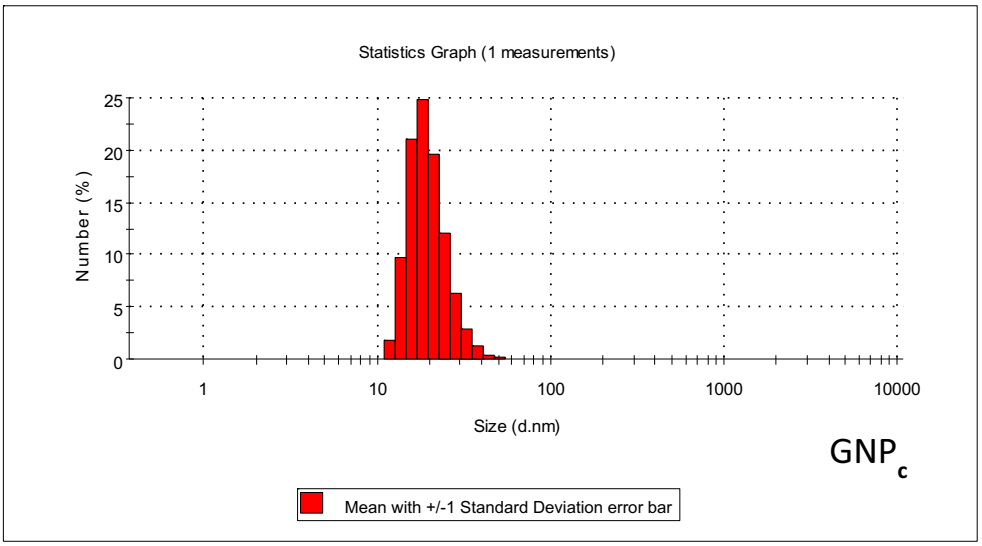

Fig. 4 Average size distribution of GNP_c by dynamic light scattering (DLS)

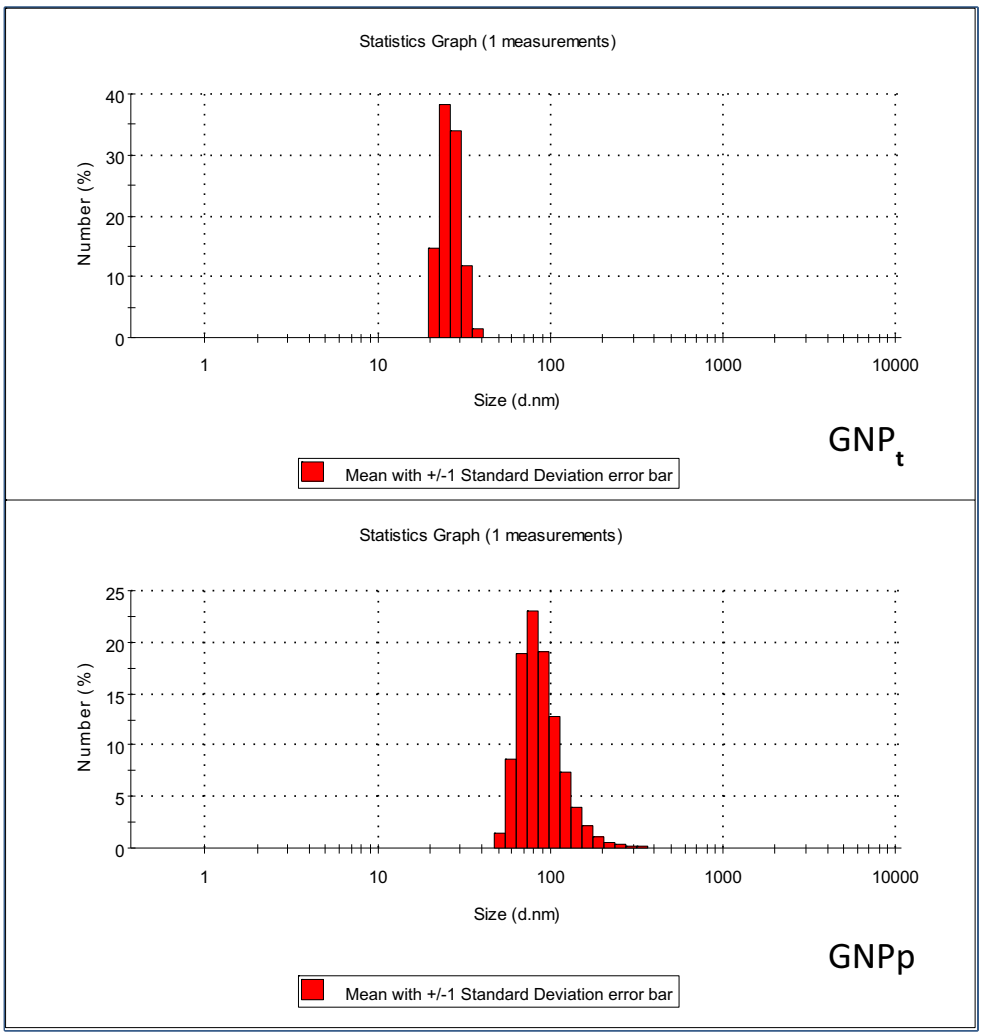

Fig. 5 Dynamic light scattering (DLS) study of GNP_t and GNP_p

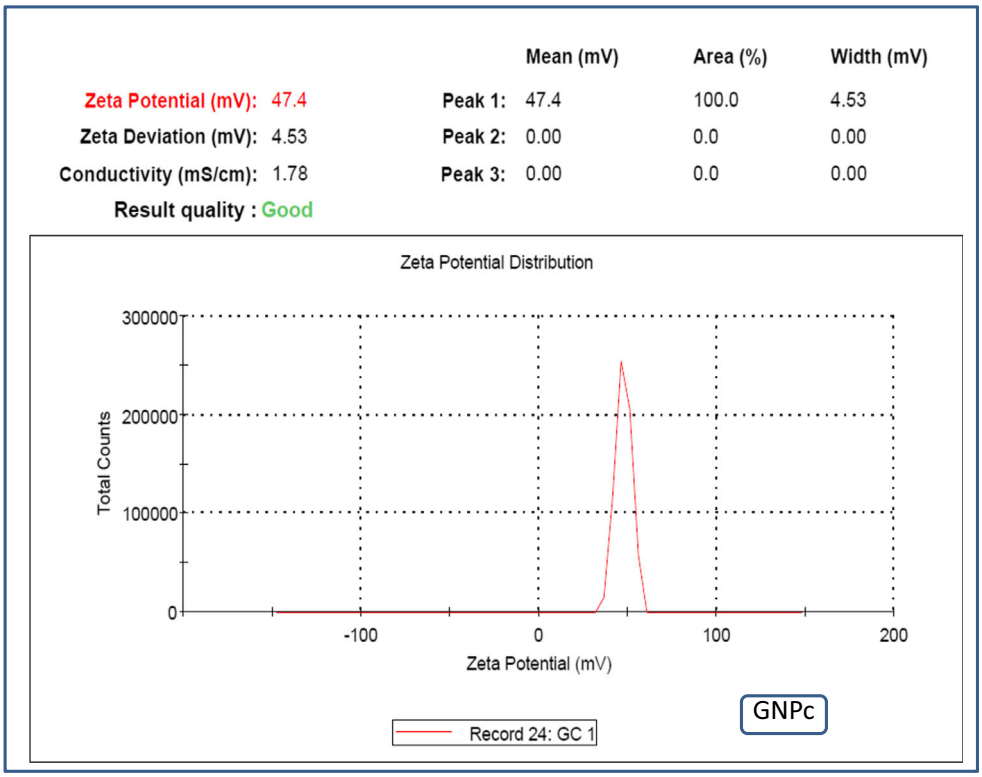

Fig. 6 Surface charge analysis of GNP_c by zeta potential measurement

2.4.3 MTT assay

Viability of exposed adult worms and mf in the concerned colloidal solutions was quantitatively assessed by the MTT reduction assay as described by Mukherjee et al. [25].

2.4.4 Measurement of ROS by enzymatic analysis

ROS such as superoxide and H_2O_2 in control and treated worms were measured following the method as described by Mukherjee et al. [23].

2.4.5 Gold particle induced apoptosis: determination of apoptogenic protein expression

A. DNA fragmentation assay Isolation of total genomic DNA from control and treated adult worms was done using the standard phenol-chloroform isolation procedure as described previously [26].

B. Western blot technique Control and treated *S. cervi* parasites were washed with PBS (pH 7.4) repeatedly and parasite homogenate was prepared following the method described previously [22]. Protein content was measured by the method of Bradford (Bradford, 1976) with some modification [22]. The obtained clear supernatant was used for Western blot and enzyme assays.

Alterations in the expression of nematode-specific apoptogenic proteins (EGL-1, CED-9, CED-4, CED-3) and housekeeping protein (GAPDH) were studied using Western blot technique as per early reports [22, 26].

C. Double staining technique AO/EtBr differential double staining was performed following the procedure depicted in our previous studies [11, 27].

2.5 Assessment of toxicity

2.5.1 In vitro cytotoxicity analysis

Toxicity of the developed materials was performed primarily in vitro upon peritoneal macrophages isolated from adult Wistar rat (160 ± 20 g) at concentrations of 30 and 75 μg/ml following a previously reported method [28].

2.5.2 In vivo toxicity analysis

For in vivo toxicity analysis, GNP samples were administered orally to a Sprague Dawley rat weighing 130 g for a period of 7 days at customary intermission. The analysis has been carried out according to the OECD guidelines [29].

Histological preparation Small portions of the freshly removed livers after perfusion were fixed in Bouin's fixative overnight, dehydrated in an ethanol series, and embedded in

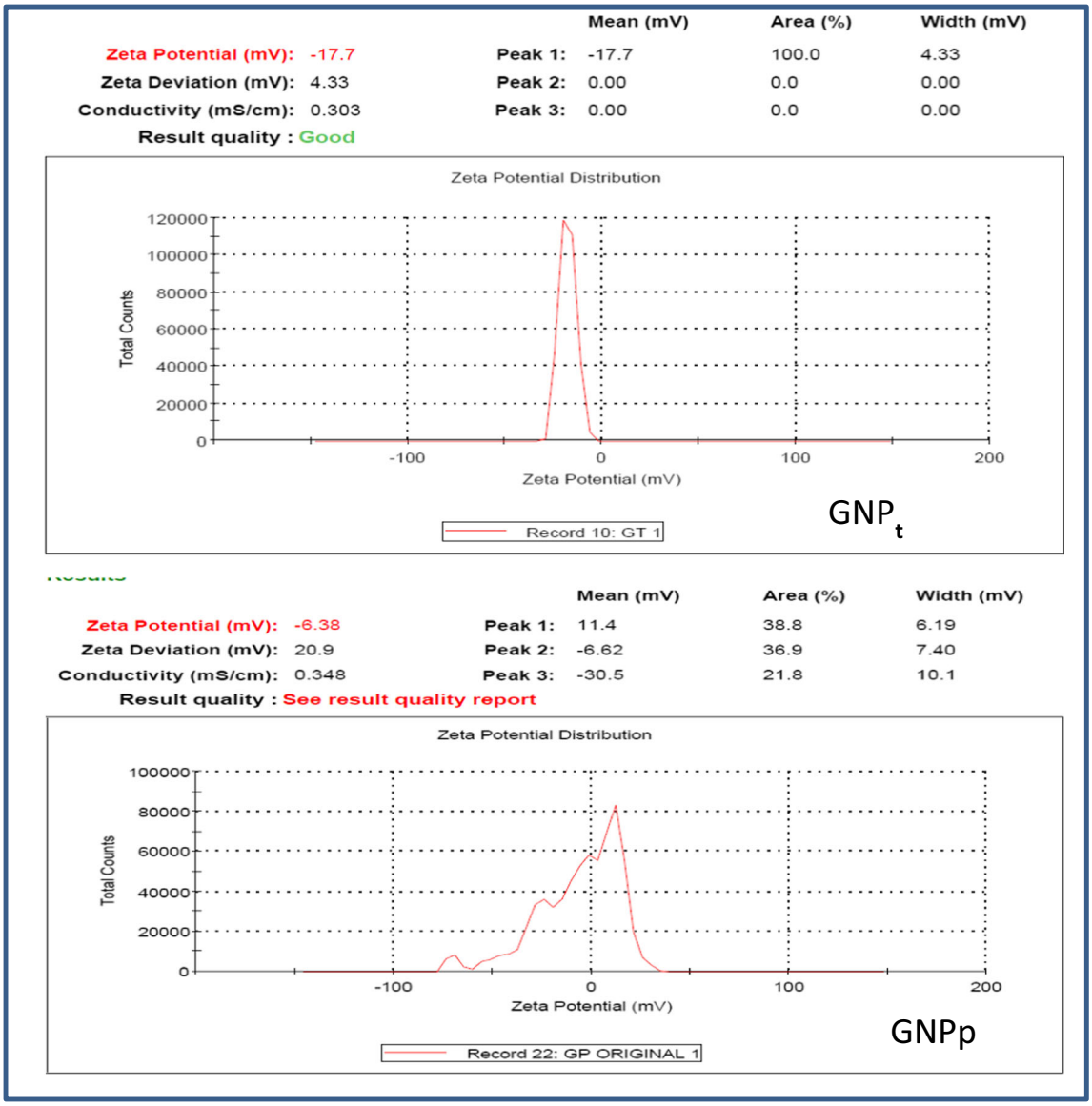

Fig. 7 Zeta potential study of GNP_t and GNP_p samples

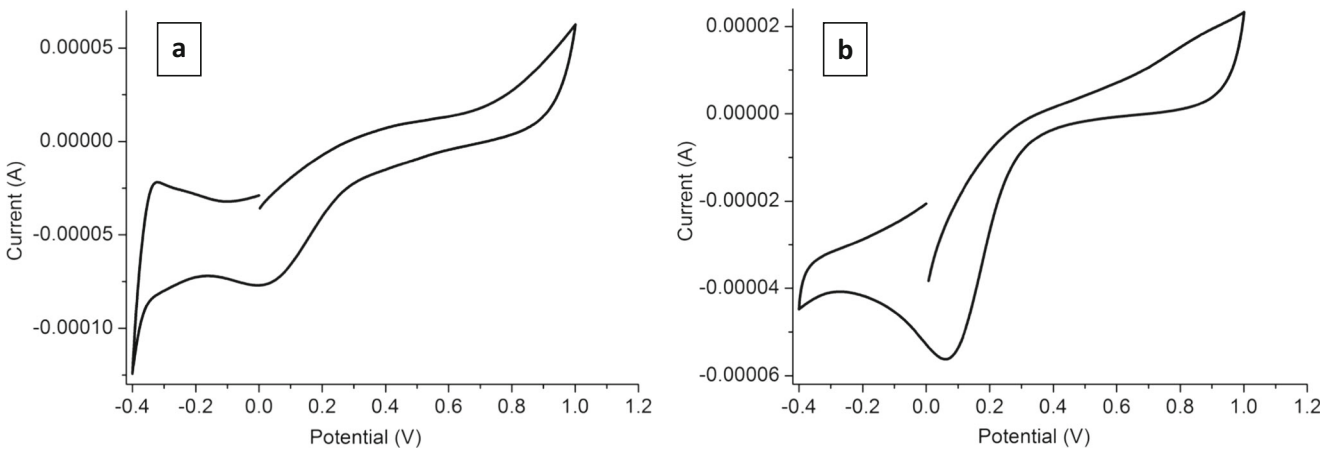

Fig. 8 Cyclic voltammograms (CV) of 1% (*v*/*v*) acetic acid solution (**a**) and chitosan in 1% (*w*/*v*) acetic acid solution (**b**) at scan rate 100 mV/s with respect to SCE (saturated calomel electrode) as reference electrode

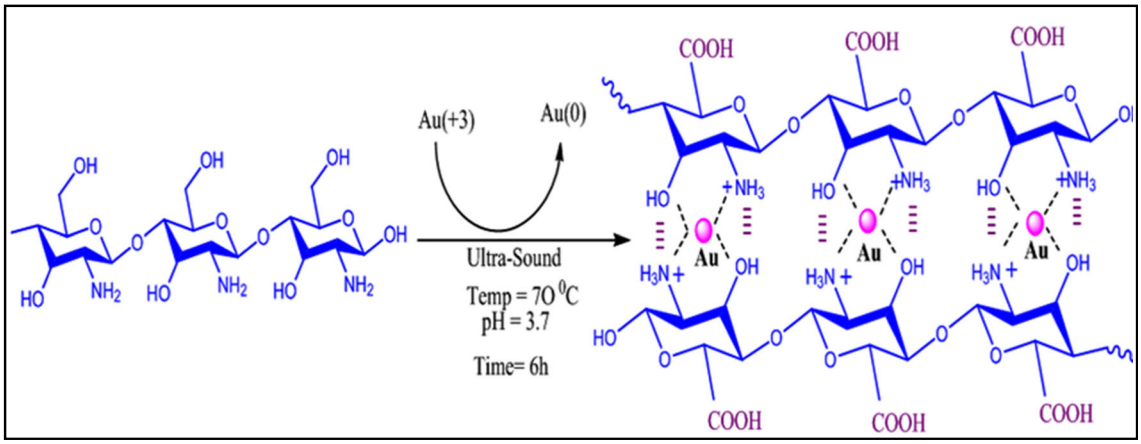

Scheme 1 Reduction-cum-stabilization effect of chitosan

paraffin wax for histological procedures. Paraffin sections (thickness 5 μm) were stained with hematoxylin and eosin (HE). Each slide was assessed for specific histological alterations under an inverted light microscope.

Determination of biochemical parameters Biochemical tests included measurement of serum total protein, albumin, globulin, total bilirubin both conjugated and un-conjugated, serum glutamate oxaloacetic transaminase (SGOT), serum glutamate pyruvic transaminase (SGPT), and alkaline phosphatase following conventional and well-established methods depicted in Mukherjee et al. [25]

3 Results and discussion

3.1 Synthesis of gold nanoparticles

The biomacromolecule chitosan, biomolecule tyrosine, and non-biopolymer PVA [30] produced gold nanoparticles with different spectral properties and stabilities. The recipes for the preparation are given in Table 1.

Due to better cohesion between chitosan and gold particle, the system (GNP_c) leads to superior quality colloidal solution. The involved scientific insight may be manifested with the help of unique reducing-cum-stabilizing property of chitosan.

3.2 UV-Vis spectra

The surface plasmon resonance (SPR) behavior of the synthesized nanomaterials was studied by UV-Vis spectroscopy. It is the consequence of resonance oscillation of conduction electron, which results in the formation of a dipole in the material due to absorption of electromagnetic waves. In the present case, all the synthesized GNPs showed intense surface plasmon absorption around 521–525 nm (Fig. 1), which is the characteristic peak of gold nanoparticles [31].

3.3 TEM and SEM study

Figure 2a, b shows representative transmission electron microscope (TEM) images recorded by drop casting gold samples on the carbon-coated copper grid. It is evident from the images that the nanoparticles were mostly spherical in shape (isotropic, i.e., low aspect ratio). The images of GNP_c revealed the average diameter of GNPs is in the 20 nm range. The dynamic light scattering (DLS) study also supported the result. Presence of well-known lattice fringe in the TEM images (Fig. 2a) and illuminated circular dotted rings in SAED (selected area electron diffraction) pattern suggest the polycrystalline nature with f.c.c. geometry of GNP [32].

To investigate the surface morphology of GNP_c, SEM (scanning electron microscopy) study was performed. The SEM image revealed the formation of prominent biopolymeric corona type structure of the nanomaterials in which chitosan formed the shell and gold particles that were incorporated in the core (Fig. 2d). Generation of this corona type of structure by chitosan answers the ultra-high stability of colloidal GNP in GNP_c. In the case of the other materials GNP_t and GNP_p, the TEM images (Fig. 3) revealed its amorphous nature.

3.4 DLS study

Dynamic light scattering study was employed to examine the average size distribution of gold particles in the three samples. GNP_t showed an average distribution around 20–40 nm range whereas GNP_c were distributed in the 10–50 nm range (Fig. 4). The broad distribution of GNP_c compared to GNP_t might be due to polymeric corona of gold nanoparticles as evidenced from SEM image. However, GNP_p showed size distribution in much higher range, i.e., 50–120 nm (Fig. 5).

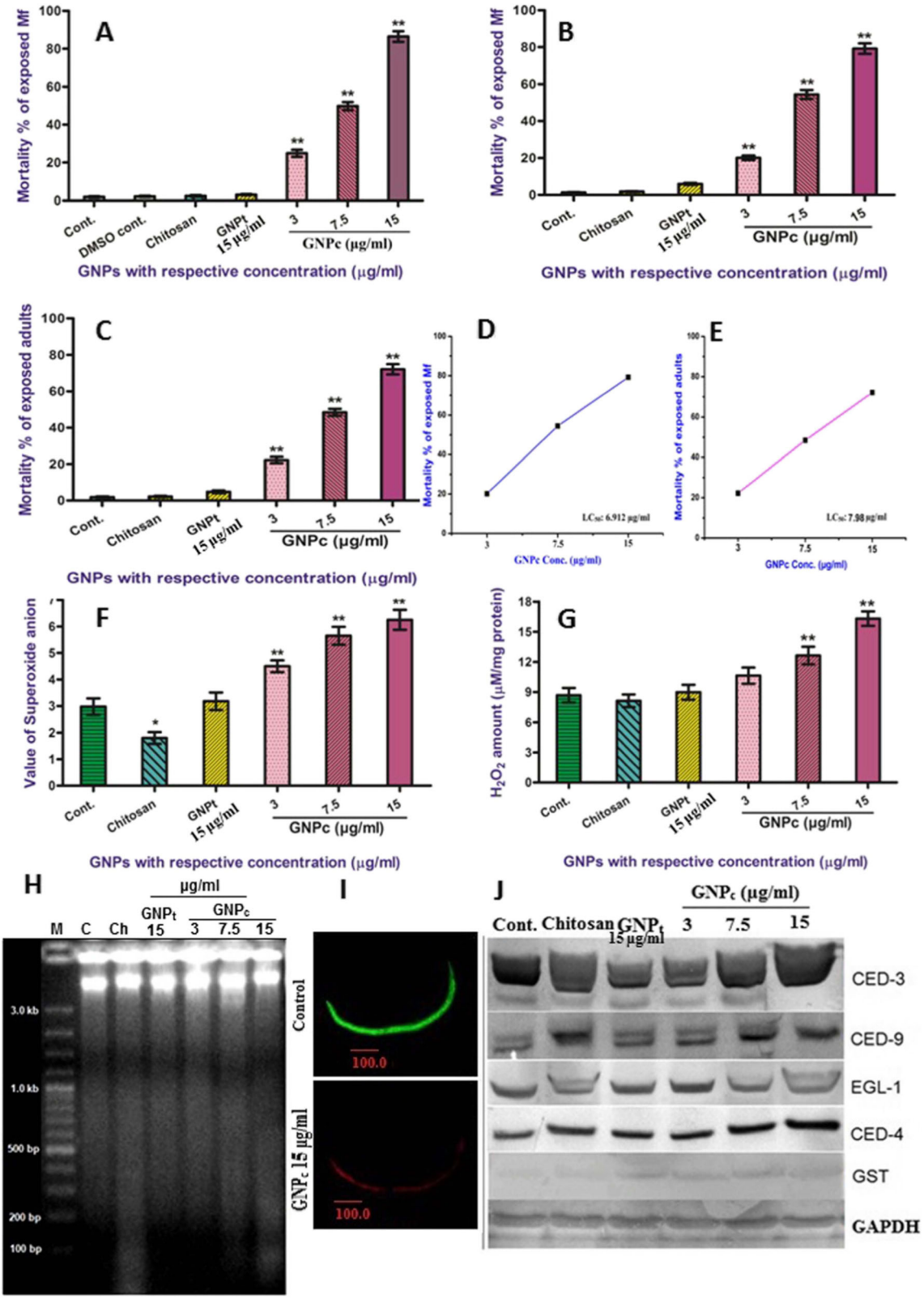
A
Mortality % of exposed Mf
Cont.
DMSO cont.
Chitosan
GNPt 15 µg/ml
3
7.5
15
GNPc (µg/ml)
GNPs with respective concentration (µg/ml)
B
Mortality % of exposed Mf
Cont.
Chitosan
GNPt 15 µg/ml
3
7.5
15
GNPc (µg/ml)
GNPs with respective concentration (µg/ml)
C
Mortality % of exposed adults
Cont.
Chitosan
GNPt 15 µg/ml
3
7.5
15
GNPc (µg/ml)
GNPs with respective concentration (µg/ml)
D
Mortality % of exposed Mf
LC50: 6.912 µg/ml
GNPc Conc. (µg/ml)
E
Mortality % of exposed adults
LC50: 7.98 µg/ml
GNPc Conc. (µg/ml)
F
Value of Superoxide anion
Cont.
Chitosan
GNPt 15 µg/ml
3
7.5
15
GNPc (µg/ml)
GNPs with respective concentration (µg/ml)
G
H2O2 amount (µM/mg protein)
Cont.
Chitosan
GNPt 15 µg/ml
3
7.5
15
GNPc (µg/ml)
GNPs with respective concentration (µg/ml)
H
µg/ml
M
C
Ch
GNPt 15
GNPc 3
7.5
15
3.0 kb
1.0 kb
500 bp
200 bp
100 bp
I
Control
GNPc 15 µg/ml
100.0
100.0
J
GNPc (µg/ml)
Cont.
Chitosan
GNPt 15 µg/ml
3
7.5
15
CED-3
CED-9
EGL-1
CED-4
GST
GAPDH

◀ **Fig. 9** Antifilarial activity of GNP_c sample. **a** Trypan blue dye exclusion test. Mortality of *S. cervi* microfilariae was evaluated after 24 h. Data were shown in triplicate (mean ± SEM) and p value < 0.05 (*) and p value < 0.01 (**). **b**, **c** Parasite mortality after the exposure of GNP_c, GNP_t, and chitosan was carried out by MTT reduction assay. **b** *S. cervi* mf were exposed to increasing concentration of these compounds for 24 h and death was estimated thereafter. **c** Mortality of *S. cervi* adults was also evaluated after the exposure of these compounds. Mortality was evaluated in comparison to untreated control. Data were shown in triplicate (mean ± SEM) and p value < 0.05 (*) and p value < 0.01 (**). **d**, **e** Determination of LC_{50} values of GNP_c. **d** LC_{50} value for mf was 6.912 μg/ml. **e** LC_{50} value for adult was 7.98 μg/ml. **f**, **g** Alteration of redox parameters. **f** An elevation in the generation of superoxide anion was notable with increasing concentrations of GNP_c as indicated. **g** An elevation in the generation of H_2O_2 was notable with increasing concentrations of GNP_c as indicated. Data were shown in triplicate (mean ± SEM) and p value < 0.05 (*) and p value < 0.01 (**). **h**, **i** Determination of apoptosis. **h** Observation of DNA fragmentation in *S. cervi* adults after 24-h exposure. Lane M denoted molecular weight marker (100–3000 bp). Genomic DNA was isolated from control and treated adults. DNA breakage was observed for treated adult parasites. Image was representative of three independent experiments. **i** Apoptosis-specific staining of microfilaria of *S. cervi*. **j** Alterations in the expression levels of apoptogenic proteins and GST in *S. cervi* adult worm lysates of control and treated. GNP_c at different concentrations (3, 7.5, and 15 μg/ml) caused a dose-dependent elevation in the expression of pro-apoptotic EGL-1, CED-4, and CED-3, and anti-apoptotic CED-9 in respect to control worms. GST activity also got upregulated for increasing concentrations of GNP_c. GAPDH served as protein loading control. For all the cases, equal amount of parasitic proteins (60 mg) was resolved. Images are representative of three independent experiments

3.5 Zeta potential measurement studies

Generally, particles with ζ-potential value more than + 30 mV or less than − 30 mV are considered to form stable dispersion due to inter-particle electrostatic repulsion [33]. GNP_c (ZP value: + 47.4 mV) (Fig. 6) showed much higher value than GNP_t (ZP value: − 17.7 mV) and GNP_p (ZP value: − 6.38 mV) (Fig. 7) which is due to the presence of cationic biopolymer chitosan. This zeta potential value goes in complete conformity with the stability physically observed for the composites.

3.6 Cyclic voltammetry study

The cyclic voltammetry (CV) was employed to investigate the electrochemical behavior of chitosan. Figure 8 shows cyclic voltammograms of 1% (*v*/*v*) acetic acid solution and chitosan in 1% (*w*/*v*) acetic acid solution at scan rate 100 mV/s with respect to SCE (saturated calomel electrode) as reference electrode. Since chitosan is soluble in aqueous acid medium, the redox behavior measurement was restricted between − 0.4 and 1.0 V window range with respect to SCE which means the value lies in between − 0.159 and 1.241 V with respect to SHE (standard hydrogen electrode). Otherwise, O_2 and H_2 will be liberated at anode and cathode respectively. Now, it is clear from the figure that chitosan has no reducing property in between the window range, but it can reduce Au(III) effectively. The E^0_{red} of Au(III) to Au(0) is 1.51 V (with respect to SHE). Thus, it may be concluded that E^0_{red} value of chitosan lies between 1.241 V and less than 1.51 V (with respect to SHE).

3.7 Mechanism of gold nanoparticle formation and its stabilization

There are several reports [34, 35] of reduction of trivalent gold to its nanoparticles by chitosan without crystal clear mechanism. So, an attempt has been made in the present work to elucidate the mechanistic path. The amine groups of the chitosan got protonated in acidic medium and the biopolymers became positively charged. When dilute hydrochloroauric acid ($HAuCl_4$) was added into chitosan solution, negatively charged Au(III) ions were adsorbed selectively on various positive centers of chitosan and the reduction process started. The reduction follows transfer of three electrons generated from the oxidation of primary alcohol groups at C_6 position of chitosan to Au(III). Thus, the overall reaction for the reduction mechanism can be expressed as Scheme 1.

In the chitosan/gold system, gold remains highly dispersed inside the polymeric matrix (Scheme 1). So, it becomes most stable. The interchange of electrostatic interactions between amino groups and hydroxyl groups in chitosan help to form the corona type structure. In contrast, tyrosine stabilized the produced gold particle by capping mechanism and finally it leads to the formation of nanoparticle. The observation was supported by TEM analysis.

3.8 Antifilarial activity

Trypan blue dye exclusion test The results of the test at different doses of GNP_c against mf of *S. cervi* for 24 h are presented in Fig. 9a. The doses at 3, 7.5, and 15 μg/ml caused death of 24.9, 49.8, and 86.4% respectively. Both chitosan itself and GNP_t exhibited no antifilarial efficacy. But significantly gold along with chitosan GNP_c manifested positive effect. Thus, chitosan and gold reinforced each other (synergistic effect) towards antifilarial activity.

MTT assay The results of the assay are shown in Fig. 9b–e). GNP_c (at the dose of 15 μg/ml) emerged as the most potent antifilarial agent as it caused 79.2 and 72.1% death of mf and adults respectively (Fig. 9b, c). Death was also prominent for other two doses of GNP_c. LC_{50} values for GNP_c against both stages of the filarial parasite were also been calculated and the values were 6.912 and 7.98 μg/ml respectively against mf and adults of *S. cervi* (Fig. 9d, e). However, chitosan or GNP_t was found to be unable at mediating death of the exposed mf or

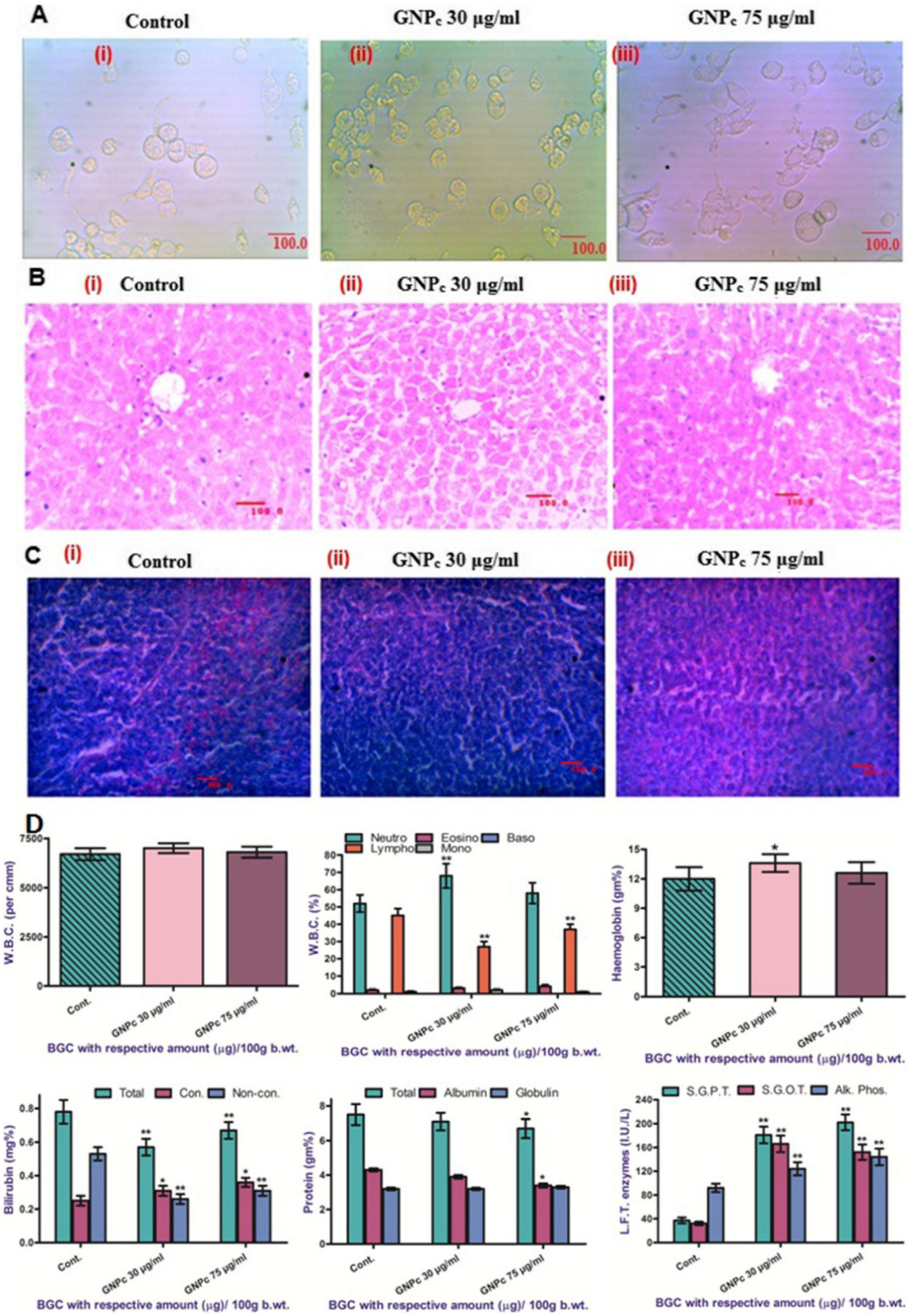
A
Control
GNPc 30 µg/ml
GNPc 75 µg/ml
(i)
(ii)
(iii)
100.0
B
(i) Control
(ii) GNPc 30 µg/ml
(iii) GNPc 75 µg/ml
C
(i) Control
(ii) GNPc 30 µg/ml
(iii) GNPc 75 µg/ml
D
W.B.C. (per cmm)
Cont.
GNPc 30 µg/ml
GNPc 75 µg/ml
BGC with respective amount (µg)/100g b.wt.
Neutro
Lympho
Eosino
Mono
Baso
W.B.C. (%)
Haemoglobin (gm%)
Bilirubin (mg%)
Total
Con.
Non-con.
Protein (gm%)
Albumin
Globulin
L.F.T. enzymes (LU./L)
S.G.P.T.
S.G.O.T.
Alk. Phos.
BGC with respective amount (µg)/ 100g b.wt.

◀ **Fig. 10** Cytotoxicity analysis. **a** In vitro cytotoxicity assessment. Phase-contrast micrographs showing control and GNP_c-treated (100 and 250 μl/ml) macrophage cells in culture. Images are representative of three independent experiments. Histological profile of representative liver (**b**) and spleen (**c**) tissues in experimental animals exposed to GNP_c (100 and 250 μl/100 g b.wt.). Liver tissues after toxicity schedule did not produce any observable alterations. Photographs were taken at × 400 magnification, scale bar = 100 μm, and were representatives of three independent experiments. **d** Serological and hematological parameters of in vivo toxicity assessment of GNP_c. Data were shown in triplicate (mean ± SEM) and p value < 0.05 (*) and p value < 0.01 (**)

adults significantly ($p < 0.05$). Thus, MTT assay confirms the observation of trypan blue dye exclusion test. It is interesting to see that the performance of GNP_c is better than its silver counterpart (in that case it was12 and 13 μg/ml respectively) [11].

ROS analysis For the evaluation of altered ROS generation in the exposed parasites, two key ROS components, namely superoxide anion (Fig. 9f) and H_2O_2 (Fig. 9g), were evaluated spectrophotometrically in the exposed adult parasites. Compared to control, GNP_c exposure to the parasites at the concentrations of 3, 7.5, and 15 μg/ml enhanced the generation of superoxide anion up to 51.0, 89.6, and 109.7% respectively. On the other hand, GNP_t (15 μg/ml) enhanced superoxide anion production to a small extent (6.7%) and, more interestingly, chitosan (15 μg/ml) lowered the production of superoxide anion by a significant 39.6%. Similarly, H_2O_2 production got upregulated by 22.5, 45.5, and 87.9% at the exposure of GNP_c at concentrations of 10, 25, and 15 μg/ml respectively. GNP_t (15 μg/ml) enhanced H_2O_2 production of only 3.3% and exposure of chitosan downregulated H_2O_2 production by 6.5%. Thus, two events happened here synchronously, where the chitosan acted as an antioxidant and gold composite prominently enhanced ROS generation. So, it can be assumed that the ROS generating property is mainly due to the gold particles only and chitosan acts as nanocarrier.

DNA fragmentation assay DNA fragmentation assay was performed in isolated DNA of control and exposed *S. cervi* adults (Fig. 9h) to detect the induction of apoptosis in filarial parasite. Most prominent DNA breakage was found in the case of GNP_c-treated parasite. The result reflected that large numbers of exposed cells died in synchrony [36]. Thus, the experimental evidence suggested that apoptosis can play a significant role in mediating death of the GNP_c-exposed filarial parasite.

Double staining test AO and EtBr strains can distinguish between living and dead mf in different stages of programmed cell death owing to varying degrees of coloration. It was observed that control mf showed green fluorescence while red fluorescent color was observed in the treated one.

Western blot analysis For the demonstration of the underlying causes of apoptosis upregulation, altered expression levels of different nematode-specific apoptogenic proteins were evaluated by Western blot analysis (Fig. 9j). Additionally, an enzymatic component of ROS cascade, GST, was also immunoblotted alongside for interpolation of ROS component in apoptosis (Fig. 9j). Although expression of anti-apoptotic CED-9 enhanced in GNP_c-treated parasites in comparison to control, other pro-apoptotic protein expressions, namely EGL-1, CED-3, and CED-4, got enhanced more prominently.

However, in the case of CED-3, changes in the expression were not prominent. The possible reason behind the peculiarity in the trend of CED-3 expression is the survival response of the parasite under the stress of nanoparticles. CED-3 is the effector caspase that is directly involved in inducing apoptotic death. Therefore, after treating with the GNPs, the possible response of the parasitic cell system was to target the effector caspase (CED-3) to escape from death. Thus, the result signified enhanced apoptosis in GNP_c-exposed *S. cervi*. GST expression got upregulated in accordance with the production of ROS in the parasites and it also signified that enhanced ROS possibly has a role in apoptosis induction.

3.9 Cytotoxicity study

Therapeutic possibility of any nanomaterials relies on the degree of cytotoxicity it exerted over non-targeted organism or tissue. Herein, our toxicity studies on GNP_c were carried out in vitro using rat. Primary macrophage cells showed negligible alteration in cell viability as well as in cell morphology (Fig. 10a). No significant changes in the histology of liver (Fig. 10b) and spleen (Fig. 10c) were noticed due to in vivo treatment of GNP_c-treated rat as compared to control. In vivo

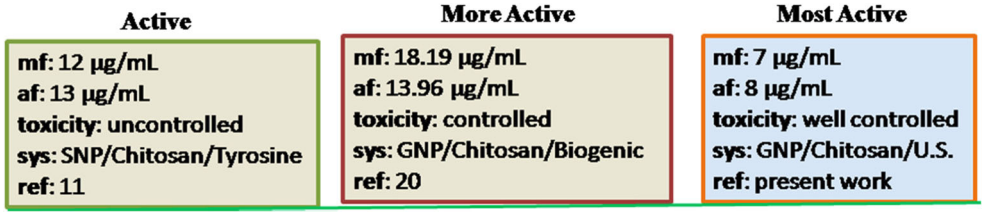

Fig. 11 Comparative antifilarial activity (in terms of LC_{50} value, μg/ml) and cytotoxicity. mf microfilaria of *S. cervi*; af adult filaria of *S. cervi*; U.S. ultrasound

toxicity analysis in Wistar rat model also showed no changes in the serum biochemical parameters (Fig. 10d). Enzymes like SGPT, SGOT, and ALP are critical marker of liver function [37]. Though significant alterations were noticed in these enzymes after 7 days continuous GNP_c treatment (30 μg/g body weights) in respect to the control group, they were within the permissible range and thus considered as safe. Therefore, the preliminary acute toxicity studies indicated that chitosan-labeled gold nanoparticles can be a safe nanoformulation for future therapeutic purposes.

3.10 Role of chitosan in improving antifilarial activity

Chitosan is especially characterized by mucoadhesive properties because of the electrostatic interaction between the positive centers ($–NH_3^+$ group at C_2 position) and the negative centers on the mucosal surfaces [38–40]. The surface positive charge of synthesized material is also evidenced from its zeta potential value (+47.4 mV). The interaction of the protonated amine groups with the cell membrane results in a reversible structural reorganization in the protein-associated tight junctions, which is followed by opening of these. The mucoadhesive nature of chitosan also increases the time of attachment at the absorption site which in turn helps in the release of nanoparticle attached with it. Hence, chitosan acts as good carrier of GNPs, which induces ROS generation in the cell. As a result, the antifilarial activities of gold nanoparticle are improved significantly.

3.11 Comparative antifilarial activity and cytotoxicity

The comparative assessments of antifilarial activity and cytotoxicity are shown in Fig. 11, which reveals that the currently developed material with the help of ultrasound (GNP/chitosan/U.S.) is the most active with respect to LC_{50} values and cytotoxicity. The present system exhibited the lowest lethal doze and the highest non-toxicity [8, 11, 20]. The salient feature further justified the concept that chitosan and gold reinforced each other towards antifilarial activity.

4 Conclusion

(i) Chemically inert gold metal was made biologically potent in its nanoform (excellent antifilarial activity with highly desirable nontoxic behavior to the normal cells) through functionalization by a biopolymer chitosan. A crystal clear mechanism has been explored for the first time to establish the role of chitosan as a unique reducing-cum-stabilizing-cum-mucoadhesive agent. The antifilarial activities of the functionalized gold nanoparticle are improved and the cytotoxicity is controlled significantly compared to the widely studied silver nanoparticle counterpart.

(ii) The designed and developed material exerted its antifilarial activity through (a) ROS generation, (b) genomic DNA fragmentation, and (c) alterations in apoptogenic protein expression.

(iii) In vitro and in vivo toxicity evaluations along with the observations of histological observation of liver and spleen stand for the non-toxic nature (i.e., alterations in histological parameters are in permissible limit) of the synthesized material.

Finally, the green and biopolymer inspired gold nanoparticles are expected to direct novel avenues in meeting the need of bioactive multifunctional non-toxic nanotherapeutic agents.

Acknowledgements We gratefully thank the financial supports provided by the CSIR (Project No. 02(0331)/17/EMR-II) and NEHU Shillong, IIT Guwahati, IACS Kolkata, for instrument facilities.

Compliance with ethical standards

Experiments with small laboratory animals were performed according to the guidelines of Committee for the Purpose of Control and Supervision of Experiments of Animals (CPCSEA), Govt. of India (1819/GO/Ere/S/15/CPCSEA).

Conflict of interest The authors declare that they have no conflict of interest.

References

1. Kumar MN, Muzzarelli RAA, Muzzarelli C, Sashiwa H, Domb AJ (2004) Chitosan chemistry and pharmaceutical perspectives. Chem Rev 104:6017–6084
2. Venkatesan J, Kim SK (2010) Chitosan composites for bone tissue engineering— An overview. Mar Drugs 8:2252–2266
3. Jain T, Kumar S, Dutta PK (2015) Chitosan in the light of nanobiotechnology: a mini review. J Biomed Res Tech 1:1–7
4. Mohammad F, Al-Lohedan HA, Al-Haque HN (2017) Chitosan-mediated fabrication of metal nanocomposites for enhanced biomedical applications. Adv Mat Let 8(2):89–100
5. Mahajan RS, Goswami K, Hande S, Bhoj P (2015) Evolution of anti-filarial therapeutics: an overview. J Microbio Antimicrob Agents 1:116–122
6. Singh Y, Srinivas A, Gangwar M, Meher JM, Misra-Bhattacharya S, Chourasia MK (2016) Subcutaneously Administered Ultrafine PLGA Nanoparticles Containing Doxycycline Hydrochloride Target Lymphatic Filarial Parasites. Mol Pharm 13:2084–2094
7. Mondal NK, Dey U, Chowdhury A, Mukhopadhya P, Chatterjee S, Das K, Datta JK (2014) Green synthesis of silver nanoparticles and its application for mosquito control. Asian Pac J Trop Dis 4(Suppl 1):S204–S210
8. Saha SK, Roy P, Saini P, Mondal MK, Chowdhury P, Sinha Babu SP (2016) Carbohydrate polymer inspired silver nanoparticles for filaricidal and mosquitocidal activities: A comprehensive view. Carbohydr Polym 137:390–401
9. Dey B, Mukherjee S, Mukherjee N, Mondal R-K, Satpati B, Senapati D, Sinha Babu SP (2016) Green silver nanoparticles for drug transport, bioactivities and a bacterium (Bacillus subtilis)-

mediated comparative nano-patterning feature. RSC Adv 6:46573–46581
10. Goswami K, Hande S, Bhoj P, Jena L, Reddy M (2014) Exploiting nanoparticle for targeted apoptosis as therapeutic modality against filarial parasite: A plausible premise. Biomed Sci 2:21–24
11. Roy B, Mukherjee S, Mukherjee N, Chowdhury P, Sinha Babu SP (2014) Design and green synthesis of polymer inspired nanoparticles for the evaluation of their antimicrobial and antifilarial efficiency. RSC Adv 4:34487–34499
12. Zafar A, Ahmad I, Ahmad A, Ahmad M (2016) Copper(II) oxide nanoparticles augment antifilarial activity of Albendazole: In vitro synergistic apoptotic impact against filarial parasite Setaria cervi. Int J Pharm 501:49–64
13. Carabineiro SAC (2017) Applications of Gold Nanoparticles in Nanomedicine: Recent Advances in vaccines. Molecules 22:857–863
14. Fu PP, Xia Q, Hwang H-M, Ray P-C, Yu H (2014) Mechanisms of nanotoxicity: generation of reactive oxygen species. J Food Drug Anal 22:64–75
15. Boyles MSP, Kristl T, Andosch A, Zimmermann M, Tran N, Casals E, Himly M, Puntes V, Huber CG, Meind UL, Duschl A (2015) Chitosan functionalisation of gold nanoparticles encourages particle uptake and induces cytotoxicity and pro inflammatory conditions in phagocytic cells, as well as enhancing particle interactions with serum components. Nanobiotechnol 13:84–94
16. Regiel-Futyra A, Liśkiewicz M-K, Sebastian V, Irusta S, Arruebo M, Stochel G, Kyzioł A (2015) Development of noncytotoxic chitosan-gold nanocomposites as efficient antibacterial materials. ACS Appl Mater Interfaces 7(2):1087–1099
17. Wang B, Chen K, Jiang S, Reincke F, Tong W, Wang D, Gao C (2006) Chitosan-Mediated Synthesis of Gold Nanoparticles on Patterned Poly(dimethylsiloxane) Surfaces. Macromolecules 7: 1203–1209
18. Dananjaya SHS, Udayangani RMC, Oh C, Nikapitiya C, Lee J, Zoysa MD (2017) Green synthesis, physio-chemical characterization and anti-candidal function of a biocompatible chitosan gold nanocomposite as a promising antifungal therapeutic agent. RSC Adv 7:9182–9183
19. Huang H, Yang X (2004) Synthesis of chitosan-stabilized gold nanoparticles in the absence/presence of tripolyphosphate. Biomacromolecules 5:2340–2346
20. Saha SK, Roy P, Mondal MK, Roy D, Gayen P, Chowdhury P, Sinha-Babu SP (2017) Development of chitosan based gold nanomaterial as an efficient antifilarial agent: A mechanistic approach. Carbohydr Polym 157:1666–1676
21. Vogel AI (1961) A textbook of quantitative inorganic analysis, 3rd Edition. 513–514
22. Mukherjee N, Mukherjee S, Saini P, Roy P, Sinha Babu SP (2014) Antifilarial effects of polyphenol rich ethanolic extract from the leaves of Azadirachta indica through molecular and biochemical approaches describing reactive oxygen species (ROS) mediated apoptosis of Setaria cervi. Exp Parasitol 136:41–58
23. Mukherjee N, Parida P-K, Santra A, Ghosh T, Dutta A, Jana K, Misra A-K, Sinha Babu SP (2016) Oxidative stress plays major role in mediating apoptosis in filarial nematode Setaria cervi in the presence of trans-stilbene derivatives. Free Rad Biol Med 93:130–144
24. Mukherjee N, Saini P, Mukherjee S, Roy P, Sinha Babu SP (2014) In vitro antifilarial activity of Azadirachta indica aqueous extract through reactive oxygen species enhancement. Asian Pac J Trop Med 7:841–848
25. Mukherjee N, Saini P, Mukherjee S, Roy P, Gayen P, Sinha Babu SP (2014) Ethanolic extract of Azadirachta indica (A. Juss.) causing apoptosis by ROS upregulation in Dirofilaria immitis microfilaria. Res Vet Sci 9:309–317
26. Nayak A, Gayen P, Saini P, Mukherjee N, Sinha Babu S-P (2012) Molecular evidence of curcumin-induced apoptosis in the filarial worm Setaria cervi. Parasitol Res 111:1173–1186
27. Dey B, Mondal RK, Mukherjee S, Satpati B, Mukherjee N, Mandal A, Senapati D, Sinha Babu SPA (2015) supramolecular hydrogel for generation of a benign DNA-hydrogel. RSC Adv 5:105961–105968
28. Okitsu K, Yue A, Tanabe S, Matsumoto H, Yobiko Y (2001) Formation of colloidal gold nanoparticles in an ultrasonic field: control of rate of gold(III) reduction and size of formed gold particles. Langmuir 17:7717–7720
29. Organization for Economic Cooperation and Development (OECD) (1995) Guidelines for testing chemicals. Repeated dose 28-d oral toxicity study in rodents, no. 407. OECD, Paris
30. Saha SK, Chowdhury P, Saini P, Sinha-babu SP (2014) Ultrasound assisted green synthesis of poly(vinyl alcohol) capped silver nanoparticles for the study of its antifilarial efficacy. Appl Surf Sci 288: 625–632
31. Shukla R, Bansal V, Chaudhary M, Basu A, Bhonde RR, Sastry M (2005) Biocompatibility of gold nanoparticles and their endocytotic fate inside the cellular compartment: A microscopic overview. Langmuir 21:10644–10654
32. Khan Z, Singh T, Hussain JI, Obaid AY, Al-Thabaiti SA, El-Mossalamy EH (2013) Starch-directed green synthesis, characterization and morphology of silver nanoparticles. Colloids Surf B 102: 578–584
33. Konkena B, Vasudevan S (2012) Understanding aqueous dispersibility of graphene oxide and reduced graphene oxide through pKa measurements. J Phys Chem Lett 3:867–872
34. Bhumkar DR, Joshi HM, Sastry M, Roy P, Pokharkar VB (2007) Chitosan reduced gold nanoparticles as novel carriers for transmucosal delivery of insulin. Pharm Res 24:1415–1426
35. Pokharkar V, Dhar S, Sastry M, Bhumkar D, Mali V, Bodhankar S, Prasad BLV (2009) Acute and Subacute Toxicity Studies of Chitosan Reduced Gold Nanoparticles: A Novel Carrier for Therapeutic Agents. J Biomed Nanotech 5:1–7
36. Rotello RJ, Hocker MB, Gerschenson LE (1989) Biochemical evidence for programmed cell death in rabbit uterine epithelium. Am J Pathol 134(3):491–495
37. Mukherjee S, Mukherjee N, Saini P, Roy P, Sinha Babu SP (2015) Ginger extracts ameliorates phosphamidon induced hepatotoxicity. Indian J Exp Biol 53:574–584
38. Sinha VR, Singla Ak, Wadhawan S (2004) Chitosan microspheres as a potential carrier for drugs. Int J Pharm 274(1-2):1–33
39. Silva AC, Nobre TM, Pavinatto FJ, Oliveira ON Jr (2012) Interaction of chitosan and mucin in a biomembrane model environment. J Col Int Sci 376:289–295
40. Ahmed TA, Aljaeid BM (2016) Preparation, characterization, and potential application of chitosan, chitosan derivatives, and chitosan metal nanoparticles in pharmaceutical drug delivery. Drug Des Dev Ther 10:483–507